Chapter 1
Bottom-up Organisation of Metallic Nanoparticles

Alastair Cunningham and Thomas Bürgi

Abstract This chapter deals with bottom-up strategies that allow one to prepare amorphous assemblies of metal nanoparticles. Within these assemblies the nanoparticles couple to each other, affecting the effective electromagnetic properties of the materials. As a consequence, besides the properties of the individual particles, parameters such as number of individual particles within the assembly, geometry of the assembly and average distance between particles within the assembly can be used to design the optical properties of a material. It is therefore highly desirable to control these parameters with high precision, which is the art of self-assembly. Compared to top-down lithographic methods the bottom-up self-assembly approach is cheap and enables the fabrication of large area two-dimensional or three-dimensional samples, making it attractive for applications. In the following, after an introduction, different strategies that were used in the past to assemble nanoparticles into defined structures are briefly discussed. Such strategies rely on templates such as liquid crystals, DNA or surfactants. A versatile approach, which relies on charge-driven self-assembly mediated by charged surfaces and polyelectrolytes, is then discussed in more detail. This approach easily allows one to build large scale amorphous layered structures of nanoparticles with high control of parameters such as distance between particles within one layer and distance between the layers. The method is not restricted to flat surfaces and can be used to coat for example silica beads, resulting in core–shell structures. An attempt has also made to rationalise the observed optical properties in terms of coupling between particles within the different assemblies, thus paving the way to the design of materials with novel electromagnetic properties.

A. Cunningham · T. Bürgi (✉)
Département de Chimie Physique, 30 Quai Ernest-Ansermet, 1211 Genève 4, Switzerland
e-mail: Thomas.Buergi@unige.ch

C. Rockstuhl, T. Scharf (eds.), *Amorphous Nanophotonics*,
Nano-Optics and Nanophotonics, DOI 10.1007/978-3-642-32475-8_1,

1.1 Introduction

1.1.1 Bottom-up vs. Top-down

The term 'nanotechnology' was first coined in 1974 [1] and since then the drive to produce structures of increasingly small dimensions and explore their unique properties has not abated. There are few aspects of modern life that do not rely on, at least in some part, the scientific breakthroughs in fabricating smaller structures that have been made in the last few decades, with nanotechnology now pervading our lives to an extent that very few, with some notable exceptions [2], could have predicted. The advances in down-scaling that have been made, have been applied to a wide range of disciplines, and have played a prominent role in the fields of information technology [3], renewable energy generation [4], medicine and health care [5]. In general, the approaches to fabricate these structures can largely be divided into two categories; top-down and bottom-up techniques [6]. The fast rate of down-scaling achieved over the last few decades, in some cases advancing at almost exponential rates, can largely be attributed to the top-down techniques, loosely defined as being the fabrication of structures from larger precursors. This can be thought of as being more of a sculpting approach, with typical examples of top-down technologies including lithographic methods, the most technologically advanced of which is arguably electron-beam lithography [7], and etching methods, which can vary from wet-chemical etches [8] to focused ion beam [9] and laser ablation [10]. While there is still an important role to be played by top-down methods, there are inherent limitations associated and these limits, if they have not been already, are on the verge of being reached. One notable drawback is the minimum feature sizes that are accessible using such techniques. In addition, such techniques tend to be cumbersome and slow, requiring prohibitively expensive equipment to produce small scale and, often uniquely, two-dimensional structures. None of these disadvantages, on the other hand, are suffered by the more novel and versatile bottom-up techniques which are increasingly being applied to produce structures of even smaller scale and more complex architecture than has previously been achievable. As the name suggests, the bottom-up approach involves the fabrication of structures from smaller units, using the properties that they possess to induce their self-assembly in the desired manner. Despite these terms first being used in connection with nanotechnology in the late 1980s this building block approach to materials synthesis, often likened to the construction of objects with Lego, is still in its nascent stage and only the surface of what is accomplishable has been scratched.

Evidence for the efficacy of these techniques can be gathered through the observation of nature, which is also seen to follow a bottom-up approach. The organisation of molecules to form progressively larger structures, from cells and DNA up to, and including, metre scale biological organisms, in a hierarchical manner show the effectiveness that such approaches can provide. Indeed the entire field of biomimetics seeks to take advantage of structures found in nature which have evolved over a long period of time and, as the name suggests, use them as models or blue-prints

which can then be reproduced using innovative chemical methods. Despite being distinct from the type of bottom-up fabrication techniques which will be discussed at greater length here, the case of biomimetics also introduces another interesting aspect of structure fabrication. In general, for useful functional structures to be fabricated, a degree of organisation must be available at two discrete levels; both at the nanoscale and at the mesoscale. After the initial self-assembly step which results in the formation of a unit, it is then typically necessary to induce, chemically or otherwise, the organisation of these units into an ordered structure which can then be used in applications. It is important to note that a perfect long range order in all three dimensions of space is seldom achieved using self-assembly techniques. However, and most importantly, in the context of the materials discussed here this is not a prerequisite for obtaining functionality or attractive electromagnetic properties. The latter are more closely linked to the properties of the individual entities and their short range ordering within larger units meaning that amorphous structures hold substantial potential. A whole host of techniques exist in the ever increasing toolkit of the materials scientist that permits both the fabrication of nanoscale materials and their organisation into larger scale architectures in a controlled manner. An exhaustive list of these is, due to the inter-disciplinary and fast-moving nature of the field, extremely difficult to produce and even more difficult to discuss in great detail. However an effort will be made to provide an introduction to some of the more important bottom-up methods with particular attention being paid to the fabrication, application and organisation of metallic nanoparticles.

1.1.2 Metallic Nanoparticles and Their Applications

The wide ranging catalogue of metallic nanoparticles which can now be routinely prepared, and in many cases are now commercially available, has garnered increasing interest as their use in a broad variety of applications has become apparent. This is largely due to their particular optical properties, more specifically the fact that they support a localised surface plasmon resonance (LSPR). This effect, which has been widely studied and documented [11], describes the coherent dipolar oscillation of the surface electrons present in a nanoparticle when excited by electromagnetic radiation of a particular frequency. This manifests itself as a strong extinction of the incident radiation which, depending on the material, exists in the visible part of the electromagnetic spectrum. The effect was first modelled by Gustav Mie in 1908 who solved Maxwell's equations for light interacting with spherical metallic nanoparticles. His equation, shown below, which includes both the scattering and absorption, holds true when dipolar oscillations of the conduction electrons are considered in the limiting case where the wavelength of the incident radiation is significantly greater than the size of the metallic nanoparticles.

$$C_{\text{ext}} = \frac{24\pi^2 R^3 \varepsilon_m^{3/2}}{\lambda} \frac{\varepsilon_2}{(\varepsilon_1 + 2\varepsilon_m)^2 + \varepsilon_2^2} \tag{1.1}$$

where

C_{ext} = extinction cross-section
R = particle radius
ε_m = dielectric constant of the surroundings
$\varepsilon = \varepsilon_1 + i\varepsilon_2$ = complex dielectric constant of bulk metal
λ = wavelength of incident radiation

Evidently, the maximum extinction occurs when $\varepsilon_1 = -2\varepsilon_m$ thus defining the position of the LSPR peak. The pioneering work which Mie executed is not limited to nanospheres and can also be modified to describe nanoparticles of other geometries such as rods [12].

These optical properties have made the use of metallic nanoparticles attractive to a number of fields interested in using them in applications. As shown in (1.1), the position of the LSPR peak is altered depending on the dielectric constant of the surrounding material. As such the particles can be thought of as probes that can accurately return information, observed as red or blue-shifts of the LSPR peak, on the refractive index, and therefore composition, of their surrounding medium. A host of sensing applications, where colour changes observed in the metallic nanoparticles can indicate trace changes in concentration of analytes, can be envisaged with many already both in use and development [13]. A comprehensive review of nanostructured plasmonic sensors can be found in Ref. [14].

One specific area of interest where sensing and metallic nanoparticles are concerned is in the field of surface enhanced Raman scattering (SERS). This effect was discovered in 1974 by Fleischmann [15] and relies on the extremely strong electromagnetic fields that exist in the nanogaps between metallic nanoparticles. This facilitates massive enhancements of the Raman signal, on the order of 10^{14}–10^{15} more than that observed under normal conditions [16], which is sufficient to allow the detection of single molecule analytes. This is extremely useful as the Raman signal can return detailed information on the vibrational levels of the analyte, allowing the technique to be used for both detection and structure determination [13]. SERS has now developed to the extent that spectra can be measured in vivo [17]. In principle this could facilitate faster acquisition times and was a significant breakthrough for the use of metallic nanoparticles in medical and biological applications. A more detailed discussion of the enhancement mechanism observed and specific SERS applications can be found in Refs. [18] and [19].

Biomedical studies of metallic nanoparticles began in the 1970s following the discovery of immunogold labelling [20]. Since then a wide array of biological sensing applications have been developed [5, 21]. Gold nanoparticles, used for medical diagnostics have even become commercialised where they form an integral part of certain pregnancy tests which are currently on the market. However metallic nanoparticles are not limited to sensing applications. One major reason for the widespread use of gold nanoparticles for biomedical applications is their relatively low

cytotoxicity which makes them particularly suitable for in vivo applications such as drug delivery [22], bioimaging [23] and cancer therapy [24]. An innovative form of cancer therapy involves suitably modified gold nanoparticles, functionalised with antibodies that recognise antigens expressed by cancerous cells and allows them to specifically bind to these cells [24]. The excitement of the LSPR through irradiation with a suitable source results in the fast conversion of the absorbed energy to heat which, as the particles are localised at the cancerous cells, is sufficient to destroy these cells whilst leaving healthy ones undamaged. In addition to the control over the surface chemistry that is required it is also necessary to push the LSPR of the nanoparticles into the infra-red region of the electromagnetic spectrum as otherwise the incident radiation used to excite the LSPR would be absorbed by the first few millimetres of skin. Infra-red radiation, on the other hand, can penetrate significantly further and facilitates the excitement of the plasmon resonance of particles that are located at the cancerous cells. By using gold nanorods, the position of whose longitudinal plasmon resonance can be readily tuned in the growth process through altering the aspect ratio of the particle, this problem can be overcome.

As well as being able to use nanoparticles in diagnostics and in the treatment of medical conditions they have also found a niche application in measuring nanoscale distances, particularly in biological samples, and can be thought of as being 'plasmonic rulers' [25]. The system is based on the strength of the coupling between a pair of metallic nanoparticles which is itself strongly dependent on the distance between them. Stronger and weaker coupling manifests itself as red and blue shifts of the LSPR peak respectively and after adequate calibration it is possible to correlate these shifts in the optical properties to the separation of the nanoparticles. Dynamic separations of up to 70 nm can be monitored allowing information on both distance and configuration to be elucidated [25]. A number of advantages exist over other methods used to determine molecular distances such as Förster resonance energy transfer measurements. Here, low and fluctuating signal intensities along with limited observation times and upper measurement limits of approximately 10 nm mean that plasmonic solutions such as the ones described may be more appropriate in certain situations [25]. However, certain issues, including the extent to which the adsorption of nanoparticles to biomolecules affects their overall structure have not been unequivocally resolved. Despite this, the power and potential that plasmonic rulers possess with respect to structure elucidation is clear to see.

An equally important field which makes use of metallic nanoparticles is that of catalysis. Despite being historically considered as merely a chemically inert metal, supported gold nanoparticles were first found to reduce the activation energy for the oxidation of CO around two decades ago [26]. The high surface area, and therefore number of active sites, provides obvious advantages. There exists a strong dependence of catalytic activity on particle size, with a large decrease in activity for particles larger than 6–10 nm being observed [26]. Therefore one of the major challenges facing the field is finding a means to maintain particle stability under the reaction conditions required. A more recent study, and direct utilisation of the plasmonic properties of metallic nanoparticles, researches the catalytic properties that are induced upon the localised heating produced when the particles are in resonance [27].

Here, a solvent mixture of ethanol and water was passed through a microfluidic cell constructed with an array of gold nanoparticles. When excited with a low power laser the heat produced at the surface of the particles was sufficient to catalyse the breakdown of the solvents and the formation of CO_2, CO and H_2 [27].

Plasmonic structures can also be used to increase the efficiencies of photochemical and photoelectrochemical processes [28]. A number of mechanisms resulting in the increased efficacy of these reactions have been proposed. For example it has been suggested that accelerated reaction rates occur due to the enhanced electromagnetic fields that exist at the surfaces of, and particularly in the nanogaps between, metallic nanoparticles by elevating the molecules involved in the reactions to excited electronic states. The metallic nanostructures essentially act as optical antennas that harvest photons and then concentrate the electromagnetic field produced to excite target molecules in the vicinity. It has also been proposed that other effects associated with excited plasmon resonances such as localised heating and mechanical oscillation may also play a role in increasing the efficiency of these reactions [28]. The first experimental observation of this effect was reported in 1983 [29] and in more recent studies remarkable enhancements of molecular excitement have been reported [30]. Such systems have potential applications in the development of organic solar cells and photoelectrochemical biosensing devices [30].

An additional application of metallic nanoparticles structured by bottom-up techniques, and of particular pertinence to the work outlined in this book, is in the field of metamaterials, where they are of fundamental importance. This term is loosely used to describe materials which possess electromagnetic properties which do not exist in nature and the application of bottom-up techniques offers the opportunity to create structures with feature sizes that would be otherwise inaccessible with traditional top-down methods. The term metamaterial, with the prefix taken from Greek and meaning literally “beyond”, first appeared in literature as recently as the year 2000 when Smith et al. published their seminal paper on a composite medium with simultaneously negative permeability and permittivity in the microwave range of the electromagnetic spectrum [31]. Since then the field has exploded, however the potential contribution that metallic nanoparticles have to make to this field is only beginning to be tapped. The down-scaling of structures which have been proven to exhibit exciting novel properties such as negative refractive indices [32], cloaking [33] and perfect lensing [34], in the microwave and infra-red regimes of the electromagnetic spectrum is necessary to push these properties into the visible range. With the obvious benefits that this would entail, increasing efforts, some of which will be outlined in the main body of this chapter, are being made to further develop the application of metallic nanoparticles to the field of metamaterials.

1.1.3 Coupling Properties of Metallic Nanoparticles

As shown, metallic nanoparticles undoubtedly have many applications, both current and future. The majority of these applications rely on the LSPR that the parti-

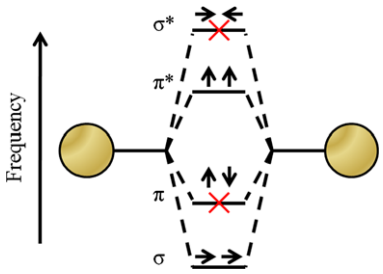

Fig. 1.1 Schematic showing hybridisation of plasmons of two approaching metallic nanoparticles. *Red crosses* indicate dark modes that only offer a weak excitation for the present configuration

cles support, allowing them to, amongst other things, sense, heat, catalyse and image. The position of the LSPR peak, as discussed above and succinctly summarised in (1.1), is dependent on a number of factors including the particle size and shape as well as the refractive index of the surrounding medium localised at the surface of the particle. However one important factor that is not considered in the equation, which analyses only a single particle, is the effect that other particles have over one another. This effect, also known as coupling, can be exploited by finding means, chemical or otherwise, to order metallic nanoparticles into specific configurations or structures. This is an additional, more flexible, method of fine-tuning the optical properties of systems and will be discussed in more detail in the following.

Coupling between metallic nanoparticles is very well summed up by plasmon hybridisation theory. This physically intuitive method, developed in 2003 by Peter Nordlander et al. [35], uses similar constructs to those used in molecular orbital theory to describe the optical changes that occur when two metallic nanoparticles are brought together to the extent where they begin to interact. The plasmonic response of a more complex structure is constructed from the interactions that exist between its constituent elements, forming hybridised modes in much the same manner that molecular orbitals are composed from the atomic wave-functions of the individual atoms that form molecules. This interaction can be considered in its simplest form as the coupling of two nearby dipoles, although depending on the size of the nanoparticles and their distance of approach higher multipole moments can also be considered. Hybridisation theory predicts two distinct classes of eigenmodes for a structure of two strongly coupled metallic spheres, i.e. a dimer. The first is associated with an in phase oscillation of the electric dipole in both spheres and is therefore termed a 'bright' eigenmode since it can radiate into the far field. The second class requires a 180° out of phase oscillation of the electric dipoles of both spheres. These eigenmodes are termed 'dark' since they cannot radiate into the far field and play an important role in the field of metamaterials as the out of phase oscillation of electric dipoles can be related in some cases to a magnetic dipole moment which is the key component in many predicted applications of metamaterials.

The method of constructing hybridised plasmonic modes through the combination of two or more resonant elements is illustrated in the plasmon hybridisation diagram shown in Fig. 1.1 and depicts the theory applied to a dimer of two metallic nanopsheres.

Shown are the individual nanoparticles with the dipoles that they support, the directions of which are dependent on the direction and polarisation of the incident

electromagnetic radiation which drives the free electrons of the metal into resonance. Similarly to molecular orbital theory these dipoles are combined in bonding and anti-bonding fashions and result in the splitting of the modes to give hybridised modes of lower and higher energy respectively. The interaction of two equal spheres results in four hybridised plasmonic modes in the coupling regime. Because of symmetry considerations, only two of these modes display a net dipole moment and will show a strong scattering of light into the far-field at relevant frequencies and angles of incidence. Conversely, both the antibonding mode for incident light parallel to the main axis of the dimer (σ^*) and the bonding mode for incident light perpendicular to the main axis of the dimer (π) have no net dipole moment and are known as dark modes (noted in Fig. 1.1 with red crosses) that can only be observed by breaking the symmetry of the system and for large spheres with extremely small interparticle distances. These dark modes contribute predominately to the absorption of the system because the resulting quadrupole moments offer only a weak coupling to the far field.

Plasmon hybridisation theory can be used to model systems both quantitatively and qualitatively and has proven to be an invaluable tool both in explaining the optical changes observed, for example spectroscopically, and in designing new systems which should have specific optical properties. It is in no way restricted to simply describing nanospheres and has been applied to nanoparticles of a wide range of different forms such as asymmetric dimers, thin metallic films, systems of metallic nanoshells, nanorods and nanostars [16]. Under certain situations it has also been shown to be applicable to large-scale systems, being used to describe the coupling between cm^2 scale arrays of metallic nanoparticles [36].

1.1.4 Bottom-up Organisation of Metallic Nanoparticles

The large potential for using bottom-up methods to organise metallic nanoparticles into assemblies that could be used as functional materials with practical applications has meant that significant amounts of research effort have been focused in this direction in recent years. Some examples illustrating the principal methods used to achieve this will be given here. As will be shown, the assembly of metallic nanoparticles relies on surface chemistry and self-assembly principles using biomolecules, surfactants, mesogens or polymers and makes use of intermolecular (interparticle) interactions. It is therefore logical that the bottom-up organisation of metallic nanoparticles is a research area where the border between physics and chemistry needs to be crossed.

Self-assembly is closely linked with the liquid-crystalline state of matter and it is therefore not surprising that liquid crystals have been used in order to organise gold nanoparticles [37]. Two principal strategies can be followed. In the first one the nanoparticles are simply mixed into the liquid crystal thus forming an physical mixture. The nanoparticles need to be functionalised in order to be stable and soluble in the liquid crystal [38]. The second strategy relies on the chemical bonding of the mesogenic unit to the nanoparticle. Whereas the first strategy is easier it often

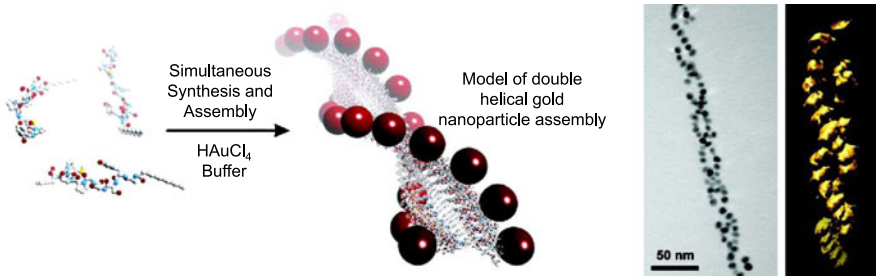

Fig. 1.2 Left-handed gold nanoparticle double helices were prepared using a method that allows simultaneous synthesis and assembly of discrete nanoparticles. *Left*: schematic principle of the method, *right*: electron microscopy images of the assembled structures. Reprinted with permission from Ref. [42]. Copyright 2008 American Chemical Society

suffers from low filling fractions. For both strategies the assembly of relatively large nanoparticles, i.e. particles that exhibit a plasmon resonance, is difficult. In some cases the metallic inclusions have been as large as 7 nm in diameter, which are large enough to support LSPRs [39].

The bottom-up assembly of metallic nanoparticles has also been further advanced through the use of biomolecules such as strands of DNA, which themselves are formed through self-assembly processes. The formation of ordered structures in such a way, using DNA as a molecular substrate for nanoparticle deposition, has facilitated the production of a number of different metallic nanoparticle architectures. One early example was the formation of dimers and trimers which was achieved through the functionalisation of gold nanocrystals with single stranded DNA oligonucleotides of defined length and sequence and assembling them on a complementary single stranded DNA template [40]. This work introduced the possibility of using oligonucleotides to self-organise metallic nanoparticles into well-defined and homogeneous structures. More recently metallic nanoparticle heterodimers comprising both gold and silver nanoparticles fabricated in a similar manner were shown to be SERS active [41]. Precise nanogap engineering was achieved through the controlled growth of silver layers on top of the original gold nanoparticles and single molecule sensitivity was shown when dyes were analysed using SERS. This advance is further evidence of such work being of fundamental importance to several fields of scientific research.

Similarly the use of a chemically modified peptide substrate to reduce a gold salt, forming gold nanoparticles along the backbone, has been shown to result in left-handed double helix arrangements of the nanoparticles (see Fig. 1.2) [42]. The introduction of chirality into structures in such a manner results in optically active arrangements of resonant elements that allow the further tuning of the optical properties of such materials.

Resting with the use of macromolecules in the ordering of metallic nanoparticles, pseudo block copolymer systems have also been employed to this end [43]. Gold nanorods selectively functionalised at their ends with polymer chains, resulting in a ‘pom-pom’ structure reminiscent of an ABA tri-block copolymer, can be

induced to organise the nanorods either end to end or side by side. This interchangeable organisation can be controlled by altering the molecular weight of the polymer chains or by simply altering the percentage composition of the solvent. The different affinities that the polymers at the ends of the gold nanorods and the CTAB molecules (CTAB: cetyltrimethylammonium bromide) along their lengths have for, for example, water, provokes the redistribution of the polymer chains and stimulates the organisation of the nanorods in different manners as the concentration of water in the predominantly organic solvent is increased. A more in-depth discussion of the ramifications that such differing organisations of gold nanorods have on the optical properties, considered through the eyes of plasmon hybridisation theory, can be found in Ref. [44].

Additional degrees of order compared with the systems previously discussed arise from the formation of binary nanoparticle superlattices from colloidal crystallisation methods which can result in impressively large crystals containing metallic nanoparticle inclusions [45]. Here, steric repulsion and van der Waals, electrostatic, and substrate–particle interactions, amongst others, all combine to determine the crystal structure where the type of control over particle size, shape and composition outlined previously allows materials with tunable physical and chemical properties to be manufactured.

It would be easy to assume, on the other hand that less ordered systems would result from the agglomeration of nanoparticles. In general this is true and such aggregation, which can occur for a variety of reasons, is normally to be avoided. However the controlled aggregation of colloidal gold nanospheres has been used to selectively produce dimers and trimers, which were subsequently used to catalyse the formation of ZnO nanowires in solution [46]. The aggregation, occurring as a result of a reduction of the electric double layer, is achieved through the addition of HCl and the particles are simultaneously stabilised by encapsulating polymers. An optimal pH for dimer formation was found to exist and high yields could be isolated upon enrichment by density gradient centrifugation. This control over the aggregation kinetics provides a route to the fabrication of ensembles with well-defined nanoparticle inclusions.

The hierarchical organisation of plasmonic nanoparticles at different length scales can also lead to interesting optical properties [47]. Such organisation has been observed within metal nanoparticle–surfactant composites, more precisely in a mixture of gold nanoparticles with triethyleneglycolmono-11-mercaptoundecylether (EGMUDE) in water [48]. EGMUDE consists of a thiol, used to anchor to the gold nanoparticle surface, a hydrophobic alkyl chain and a hydrophilic ethyleneglycol part. After addition of EGMUDE to preformed GNPs a fast colour change from purple to dark blue and sedimentation is observed, which is usually indicative of nanoparticle agglomeration. However, after some time (several hours without shaking) the sample changed colour again. UV-visible spectra showed a strongly red-shifted plasmon resonance (see Fig. 1.3) and dynamic light scattering revealed the formation of larger amorphous assemblies of gold nanoparticles, which was then also confirmed by transmission electron microscopy (TEM, see Fig. 1.3). These entities represent hierarchical structures composed of gold nanoparticles clustered

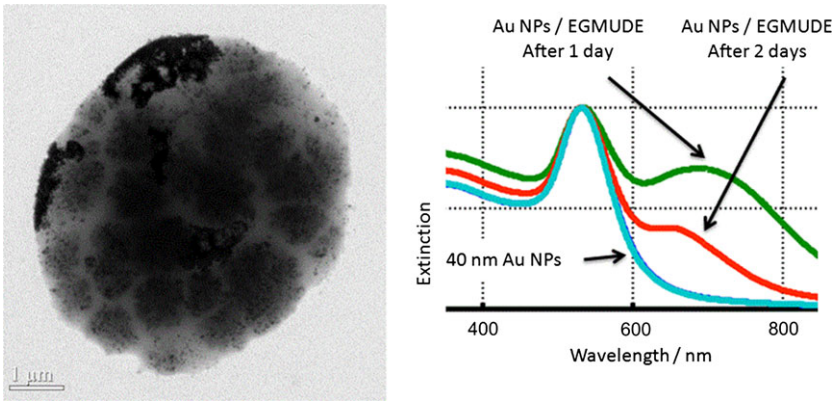

Fig. 1.3 Transmission electron microscopy (TEM) image and UV-vis spectra of gold nanoparticle (40 nm) EGMUDE assemblies [48]. Reproduced by permission of the PCCP Owner Societies

together into larger aggregates of about one micron. Several of these entities again cluster together to even larger units. The assembly of the nanoparticles is guided by the EGMUDE, which also stabilises the particles. In order to better understand the optical response calculations were performed on analogous structures by applying analytical solutions of Maxwell's equations for particles with a spherical symmetry, well-known as Mie-theory, which was extended to handle aggregates of spheres [49]. With this method one can calculate all quantities of interest for clusters consisting of arbitrarily arranged nanoparticles with a spherical shape. Such calculations very well reproduced the shifted plasmon resonance and furthermore indicated that the dominating contribution to this spectral feature arises from a magnetic dipole oscillation that is induced due to the spherical shape of the fabricated supramolecular clusters.

By combining top-down and bottom-up techniques it is also possible to exploit the advantages of both, resulting in substrates with metallic nanoparticles that self-assemble into structures that also exhibit long range order. Two-dimensional square arrays of gold nanoparticle clusters can be prepared, for example, by inducing their template directed self-assembly into holes prepared by laser interference lithography [50]. These hybrid techniques can be implemented when required and provide an additional layer of flexibility when it comes to preparing structures of a particular design.

This introduction has given a small snapshot of some of the principal bottom-up self-assembly routes towards nanoparticle organisation and is by no means comprehensive. As shown, the field of bottom-up assembly of metallic nanoparticles is considerably developed in terms of what is achievable and the wide range of methods that exist to accomplish design goals set. However, at the same time the continual introduction of new techniques and their combination with existing ones means that this is an extremely fast moving area of research that makes notable advances on an extremely quick basis. This means that only the surface has been scratched in

terms of what can be achieved with respect to metallic nanoparticles structures and highlights both the power and versatility of the techniques discussed.

Of course, one of the principal advantages of the bottom-up approach is its flexibility and often a combination or variation of one or more of the techniques discussed above is required to achieve the desired results. Indeed, one could argue that problems of either a scientific or practical nature should be considered on a case by case basis when searching for bottom-up solutions. As such, the power of the bottom-up approach will be illustrated in this chapter through the detailed discussion of two particular examples in more detail which exemplify the control which can be achieved at both length scales introduced above; the nanofabrication of metallic nanoparticles using colloidal nanochemistry and their mesoscale organisation using surface chemistry and polymer self-assembly techniques. These case studies, showing the fabrication of layered arrays of metallic nanoparticles and core–shell nanoclusters, will demonstrate that both size and structure can be at least equally as important as composition in terms of tailoring the optical properties of such materials.

1.2 Manipulation of Metallic Nanoparticles at the Nanoscale

For the metallic nanoparticles discussed in the introduction to be of any practical use, for example in the construction of metamaterials with specific properties or functional optical devices, they must first be incorporated, or organised, into structures which take advantage of the particular optical properties that they possess, of which the most important is the exhibition of an LSPR [51]. The fabrication of these particles can be traced back several centuries from when they were used to give stained glass ornaments and windows their characteristic hues [52]. The beginnings of this field in true scientific terms, however, was in 1857 when Faraday, thought of by some as being the father of modern nanoscience, first prepared and characterised colloidal gold nanoparticles in a controlled manner [53]. Very similar methods [54] to that which Faraday developed are still currently used to produce nanoparticles although today a much larger gamut of preparation techniques can now be drawn upon by modern materials scientists to prepare a wide variety of nanoparticles of differing shapes, sizes and materials [55, 56]. However, merely synthesising a batch of metallic nanoparticles, whilst interesting in its own right, is not sufficient in order to fully exploit their optical properties. For this to be achieved it is first necessary for a degree of control to be assumed over a number of important material parameters, not least of which is the morphological organisation of the nanoparticles at the nanoscale. This is where the major challenge lies for nanochemists looking to make advancements in the field. The development of novel and innovative methods combined with the exploitation of pre-existing ones is vital if the manipulation of metallic nanoparticles at this scale is to be successfully realised. Yet even the large degree of control over geometrical arrangement, which can now be routinely realised with impressive results using techniques such as electron beam lithography [57] and direct laser writing [58], is not entirely sufficient where the fabrication of

functional optical devices is concerned. For this to be accomplished it is also necessary to be able to expand such structures to utilisable scales in each dimension. In the modern world the importance of the efficient fabrication of large area, homogeneous structures is self-evident with the ubiquitous financial constraints that exist. In addition, the expansion of such structures into the third dimension is equally important if metamaterials with effective medium parameters are to be realised [59].

As mentioned in the introduction, a single solution to both of these problems is to use a bottom-up approach whereby small building blocks, in this case metallic nanoparticles, are coerced, through the application of chemical techniques, into self-organising into desirable structures. Of course, as with any emerging field, there remain some difficulties with employing this approach which are unavoidable. The loss, or reduction, of order that is achievable through the use of more traditional nanofabrication techniques makes the modelling of the optical properties of such materials significantly more challenging. However this loss of order can also be considered as advantageous as strong spatial dispersion hampering the unambiguous introduction of effective material parameters is no longer an issue. Additional benefits that arise through the application of the self-assembly route include the fabrication of previously inaccessible feature sizes [60], the facile and homogeneous deposition of nanoparticles onto large scale (cm^2) substrates [36] and the ready possibility of extending structures into the third dimension [36]. These advantages largely outweigh any disadvantages that exist and allow the preparation of larger scale structures constructed from smaller scale resonant elements at significantly reduced costs. Prior to devising fabrication routes it is first necessary to have an architecture in mind that would be of interest to the community. These are generally conceived in collaboration with theoreticians and this design process, which is outwith the scope of this chapter but discussed in detail in other chapters of this book, generally results in a trade-off between what is structurally desirable and what is presently technologically achievable.

As previously mentioned, the primary reason that metallic nanoparticles are of such interest is that they can support an LSPR at optical frequencies. The optical properties of an ensemble of two or more of these particles, approaching to within certain well-defined distances, can be significantly affected [16]. This effect, known as coupling, allows the LSPR to be manipulated and tuned with a high degree of control and gives rise to a new range of materials classed as plasmonic molecules. One such design that takes advantage of this effect is layered arrays of amorphously arranged metallic nanoparticles separated by well-defined and controllable distances. Structures such as this can be fabricated using true bottom-up approaches [36, 61] or, with less precision, through the use of other deposition techniques such as spin-coating [62].

1.2.1 Gold Nanoparticle Preparation

One method that can be used to deposit an array of, for example, gold nanoparticles on a large scale planar substrate such as glass or silicon is to exploit the inherent surface charge that exists on the particles when produced by the Turkevich

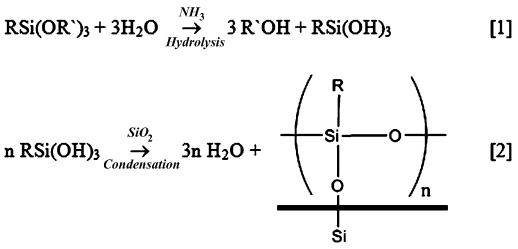

Fig. 1.4 Two step substrate functionalisation process using silica chemistry

method [63]. This method is generally accepted as being one of the most efficient means to produce spherical, monodisperse gold particles with a size range in the order of 9–120 nm in diameter [64]. Their distinctive surface charge arises from the citrate molecules which fulfil two important roles in the particle growth reaction. They firstly reduce the gold ions present in solution to produce atomic gold and secondly cap the particles that are produced, forming a protective monolayer at the surface which prevents their aggregation due to the repulsive forces generated between two like-charged particles. The negative surface charge of the particles results from deprotonated carboxylic acid groups within the molecule and is therefore clearly pH dependent. The citrate molecules, or rather their concentration relative to that of the initial gold salt, are also crucial in determining the overall size of the particles with greater relative concentrations of citrate resulting in smaller particles and *vice versa*, the greater specific surface area exhibited by smaller particles necessitating more citrate molecules to completely encapsulate all of the particles.

1.2.2 Substrate Functionalisation

In order to induce an electrostatic attraction between the gold nanoparticles and any substrate the surface of this substrate must necessarily possess an opposite charge, in this case positive. Glass and silicon, perhaps two of the most useful substrate materials, in terms of availability, cost and perhaps most importantly ease of characterisation and functionalisation, do not, however, exhibit a strong charge. As such, prior to the deposition of any particles, it is first required that the surface chemistry of the substrate be modified in such a way that a positive charge be exposed at the surface. This is readily achievable through the application of what is known as silica chemistry, a topic that has been comprehensively documented by Ralph Iler in his book: *The Chemistry of Silica: Solubility, Polymerization, Colloid and Surface Properties and Biochemistry of Silica* [65]. In brief, a suitable substrate, which has first undergone a rigorous cleaning procedure involving piranha solution, such as the ones under discussion here can be modified in a facile two-step reaction. In the first step a trifunctional organosilane for example, a trimethoxy- or trichlorosilane is hydrolysed to a silanol in what is a base-catalysed reaction. The silanol molecules then undergo a condensation reaction with the hydroxyl groups at the surface of the substrate to form a network, as illustrated in Fig. 1.4, which can be set in place using a baking step.

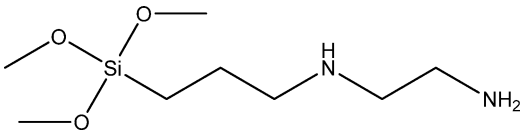

Fig. 1.5 *N*-[3-(Trimethoxysilyl)propyl]ethylenediamine—an example of a typical silane compound used to functionalise glass and silicon substrates. Following functionalisation the terminal amine group is exposed and completely alters the surface chemistry of the substrate

An enormous degree of flexibility exists here due to the wide range of silane compounds that are either commercially available or are relatively easy to prepare. In this specific case a trimethoxysilane with a terminal amine group, shown in Fig. 1.5, was chosen. At neutral pH this group is protonated, thus inducing the required electrostatic attraction between substrate and particles.

1.2.3 Fabrication of Gold Nanoparticle Arrays

When such a substrate, functionalised in such a manner, is exposed to a solution of gold nanoparticles the attractive forces between the two results in the particles adsorbing over a period of several hours until they form a complete array of well dispersed and approximately equally spaced resonant entities at the surface. A glass substrate which has such an array of gold nanoparticles adsorbed at the surface displays a characteristic pink colour which originates from the strong extinction peak that exists at around 520 nm—the LSPR wavelength. An example of this is shown in Fig. 1.6a. The colour is surprisingly strong, given that only a single layer of nanoparticles, with a diameter of around 20 nm, has been adsorbed at a relatively low density or filling fraction. The filling fraction of particles at the surface is again governed by the electrostatic repulsion that exists between them and prevents a second particle from closely approaching one that is already adsorbed at the surface. The particles, which are at least to some extent mobile at the surface, are capable of rearranging to find an organisation representing a low energy state. This is of course why, post-deposition, we observe the particles at reasonably well defined distances from one another, as can be observed in the SEM micrograph shown in Fig. 1.6b. No long range order, however, is perceived which, as can be expected, is due to the random adsorption processes. The amorphous order observed, however, is largely outweighed by other advantages. The only limitations in terms of overall substrate size that can feasibly be coated that exist are of a practical nature. The arrays are virtually defect free and as such this technique quite easily lends itself to applications on relatively large scales.

Detailed analysis of the SEM micrograph shown in Fig. 1.6b using image processing programs such as *ImageJ* [66] allow such arrays to be more fully characterised. It is possible to count thousands of particles over relatively large areas to achieve accurate average values for important material parameters such as particle

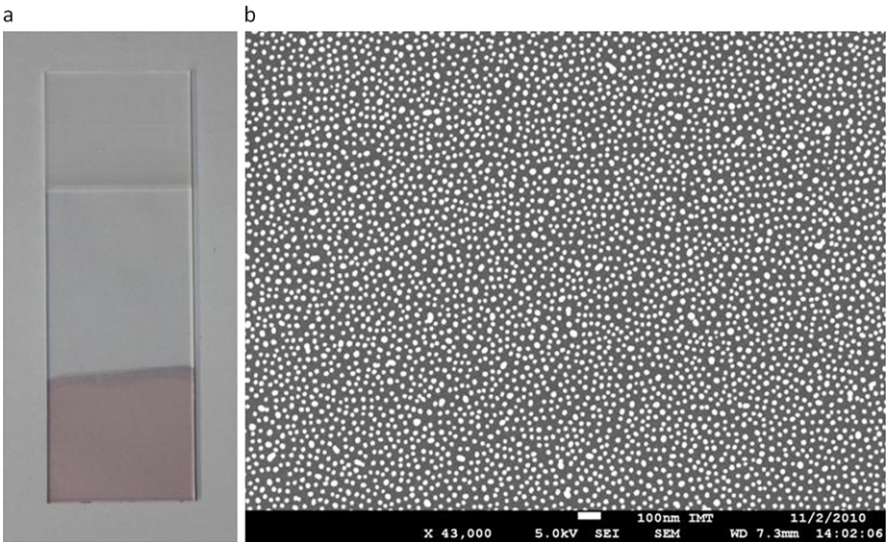

Fig. 1.6 (**a**) Photograph of single array of gold nanoparticles deposited on a functionalised glass microscope slide. (**b**) Corresponding SEM micrograph showing organisation of a single array of gold nanoparticles on a Si substrate which had been previously functionalised

density and size. Such an analysis reveals that the particles deposit at the surface with an average density of around 850 particles/μm^2 which equates to a filling fraction of 27 % [36]. While such a relatively low surface coverage can result in a strong colouration of substrates there may be instances whereby it could be desirable to have surfaces that were coated to either a greater or lesser extent. For example some simulations [67] suggest that for a sufficiently high dispersion to be achieved the filling fraction of arrays of metallic nanoparticles, such as the one under discussion here, should be higher than 30 %. For smaller filling fractions the large magnitude of the permittivity, necessary to observe Mie-resonance for sufficiently small spheres, is not achieved.

1.2.4 Controlling Nanoparticle Density

Lower density arrays are relatively straightforward to produce. As the deposition process occurs over a relatively long time-scale it is sufficient to merely reduce the number of interactions that occur between particles and substrate to create arrays with a lower filling fraction. This can be accomplished in a variety of manners, perhaps most simply by either diluting the solution from which the gold nanoparticles are deposited, or reducing the deposition time.

Creating gold nanoparticle arrays of higher density, on the other hand, is not as straightforward and requires a more considered approach. As previously mentioned,

the primary barrier to a closer packing of the particles at the substrate is the negative charge that they possess, introducing an electrostatic repulsion between them. In order to induce a higher filling fraction a means of removing or mitigating, at least partially, this repulsion must be found. One option available is through the careful regulation of the electric double layer that exists in the volume surrounding each nanoparticle [68]. The electric double layer can be defined as the volume of solution containing an excess of ions which balance the surface charge. This volume can itself be considered as being composed of two distinct regimes: the *Stern layer* which denotes the molecular layer of ions of an opposite charge to that of the surface; and the *diffusive layer* which extends into the bulk of the solution. The distance that the electric double layer extends from the surface of the gold nanoparticles is governed by a number of factors including temperature, pH and, importantly, the concentration of ions in solution. Factors such as these ultimately control the maximum density of particles that can be deposited on a charged substrate. For example, the addition of salt to the gold nanoparticle solution contracts the electric double layer and arrays of higher filling fraction are obtained. On the other hand, by reducing the concentration of ions in solution using techniques such as dialysis or centrifugation, the electric double layer would expand and lower density arrays result.

Rather than reducing the mutual repulsion between nanoparticles by regulating the distance that the electric double layer extends from their surface an additional approach is the removal, at least to some extent, of the citrate molecules that cause this repulsion in the first instance. One means of realising this is through making use of the strong sulphur—gold bond and the high affinity that thiol molecules have for gold [69]. When an array of gold nanoparticles is exposed to a solution of thiol molecules a proportion of the citrate capping molecules, largely dependent on the relative concentrations of the two ligands, will be replaced in an exchange reaction. As such, the pre-existing negative charge on the particles is, at least partially, removed along with the barrier to closer approach and reorganisation at the surface [70]. This part replacement of the citrate molecules which previously formed a protective shell at the surface of the nanoparticles results in a number of changes which can be observed in terms of the organisation and morphology of the gold nanoparticle array. Disadvantageously, a number of gold nanoparticles are solubilised and desorb from the surface as their electrostatic attraction to the substrate is diminished. This, due to the high affinity that the thiol molecules have for gold, is unavoidable. However, the same removal of charge which causes this desorption of a small proportion of the nanoparticles also induces a reorganisation of the ones that remain at the surface. This has a number of consequences in terms of changing optical and morphological characteristics of the sample as well as opening up a number of possibilities with respect to a flexibility of structure fabrication and meeting design goals. Where previously, as shown in Fig. 1.6b, an array of well-separated gold nanoparticles is formed, when the barrier to reorganisation has been removed the particles increase in mobility and tend to aggregate into small chains and clusters of around 5–10 particles. This process is thought to be driven by the energetically favourable, formation of bilayers of the relatively long alkyl chains that form the second functionality of the thiol molecules employed in this work, namely

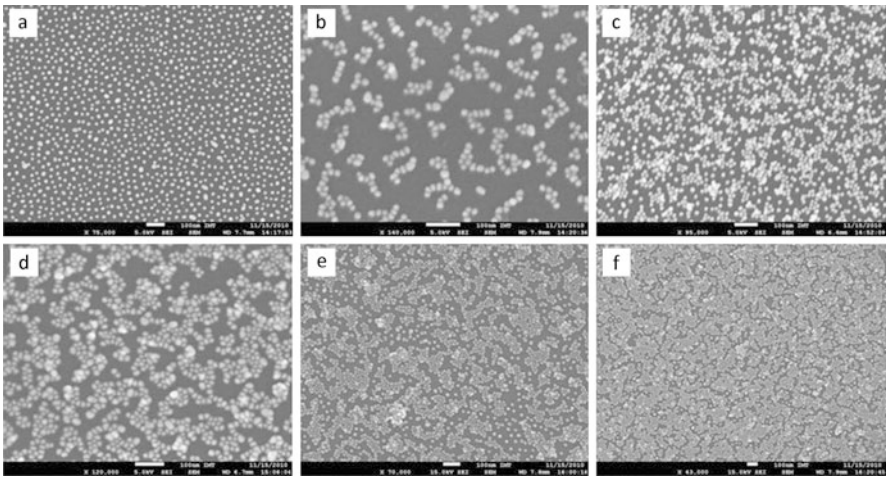

Fig. 1.7 SEM micrographs depicting various stages of the deposition and reorganisation process as *described in the main body of the text*. Shown are the morphology that could be expected after (**a**) the first deposition, (**b**) the first reorganisation, (**c**) the second deposition, (**d**) the second reorganisation, (**e**) the third deposition and (**f**) the fourth deposition. An increase in particle density as well as the introduction of a degree of order can clearly be observed

1-dodecanethiol. Crucially, any coalescence of the particles is prevented by the bilayers of the thiol molecules that are formed as they are drawn together which is essential in terms of maintaining the LSPR that they exhibit. The thiol molecules, or more importantly the length of the alkyl chain, also determine the closest distance to which the gold nanoparticles can approach one another which in this case is on the order of 1–2 nm. A by-product of forming these clusters, along with the desorption of a limited number of particles, is the appearance of large areas of void space at the surface of the substrate. Where previously the particles were well-dispersed and equally spaced indicating that a steady state had been reached and a maximum surface coverage, under these particular conditions, had been attained this is now clearly not the case. It is possible, as the void areas at the surface remain functionalised with the silane compound, to subject the substrate to a second deposition process, thus filling in these areas with arrays of particles identical in morphological form to that of the original. This array will in turn, if exposed to the same thiol solution, undergo an identical mobilisation and reorganisation process, forming larger clusters of closely packed gold nanoparticles. This process can be easily followed using scanning electron microscopy, as shown in Fig. 1.7, and if repeated several times results in a much higher density array of gold nanoparticles which, in small domains at least, are organised in a close-packed manner. This is clearly a significant improvement on the previous situation if higher density arrays of metallic nanoparticles are required to give, for example, specific optical properties.

The increase in filling fraction and order after this process is carried out is clear to the eye when SEM images are compared and contrasted. However, it is also possible to quantify these changes by analysing the micrographs using the image processing

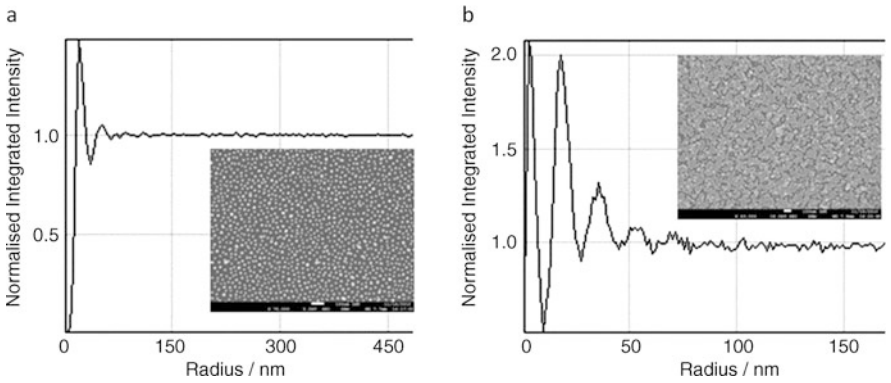

Fig. 1.8 Radial distribution functions (**a**) before and (**b**) after reorganisation and deposition processes. The corresponding SEM micrographs are shown in the *insets*

program *ImageJ* [66]. Figure 1.8a shows the radial distribution function for a low density array of gold nanoparticles before it has undergone the reorganisation and deposition process while Fig. 1.8b shows the radial distribution function after 5 cycles of reorganisation and filling have been completed. In both cases the corresponding SEM image is shown in the inset. The radial distribution function is a means of measuring the correlation between particles within a system or, more specifically, a measure of, the probability of finding a particle at a distance r away from a given reference particle. A peak indicates an increased prospect of finding particles at that given distance from a central reference particle while an intensity of 1 corresponds to the average particle density. An intensity of less than one reveals that there is a diminished probability of finding a particle at this distance. Focusing on the low-density situation shown in Fig. 1.8a and considering moving radially away from a central reference particle several important features can be noted. Firstly, the trough at short distances indicates that, as expected, there is a low probability of finding particles, which are amorphously arranged, close to others. One prominent peak, at a distance which corresponds to the average separation between any given particle and its nearest neighbours, is then observed before another trough corresponding to a second region of reduced probability is seen. Outwith this radius the distribution function tends to 1, showing that no additional order can be discerned. Two important differences can be noted, however, in Fig. 1.8b. Again moving radially away from a central reference particle it can be seen that the first peak occurs at a much smaller distance. This is a mark of closer packing and a good indicator of overall filling fraction. Secondly, several, perhaps as many as 5, peaks can now be discerned, showing that there is a considerable increase in the order observed in this sample.

The morphological changes described, at each stage of the process, result in significantly differing optical properties that can be tracked by UV-vis spectroscopy. The individual particles in the case of the low density array are suitably well-separated and have no significant influence over one another. The strength of coupling decreases exponentially as two resonant particles are moved away from one

another and an appreciable interaction is only observed when they are brought to within a distance of approximately one particle diameter. As such, in the low density case the optical properties of the array are not substantially different from that of the individual particle. However, upon each reorganisation step, in the process of fabricating structures of higher filling fraction, nanoparticles are brought to within this coupling limit, therefore altering the optical properties. This is manifested as a significant red-shift of the LSPR of up to 100 nm over 5 reorganisation steps.

1.2.5 Extending into Third Dimension—The Bulk-Assembly of Polyelectrolyte Layers and Multiple Gold Nanoparticle Arrays

As has been shown, a significant amount of control is afforded over the organisation of gold nanoparticles within a single planar array. However, for a variety of applications it is also extremely desirable to extend these gold nanoparticle arrays into the third dimension. A suitable technique for achieving this is through the build-up of layers of charged polymers, or polyelectrolytes, which exploit the same electrostatic forces that were originally used to deposit the nanoparticles on the substrate [71]. A wide range of polyelectrolytes, each with their own specific properties, exist [72]. However, two typical polymers chosen for their versatility, and the ones used in this work are the anionic poly(sodium 4-styrenesulfonate) and the cationic poly(allylamine hydrochloride). The process of polyelectrolyte deposition necessitates a charged surface of some description. In the case under discussion here this charge comes from either the silane functionalised substrate or the gold nanoparticles themselves. When the surface is immersed in a solution of the polymer the polymer becomes bound through multiple electrostatic interactions. A monolayer is formed and excess charge on the exterior allows, after a washing step to remove any excess, the process to be repeated through immersion in a solution of oppositely charged polymer. This deposition and wash cycle can be repeated as many times as required with the possibility of building up truly three dimensional systems realised. Arrays of gold nanoparticles can be included at any stage of the process, the only prerequisite being, of course, that they be sandwiched by polymers of an opposite charge. The minimum array separation is therefore imposed by the thickness of one polymer layer which is thought to be on the order of 1–2 nm [36, 61, 73]. A graphical representation of a similar system to that described above is shown in Fig. 1.9.

Additionally, the finite thickness of each polymer layer, which is itself dependent on a number of factors such as polymer type, ionic strength of the solution and molecular weight, allows thin films of extremely precise thicknesses to be constructed. This has obvious implications when used in combination with gold nanoparticles of finite separation as the coupling strength, and therefore the frequency of the LSPR are largely dependent on the distance between them. Although the situation is slightly more complicated, this holds true when large scale arrays,

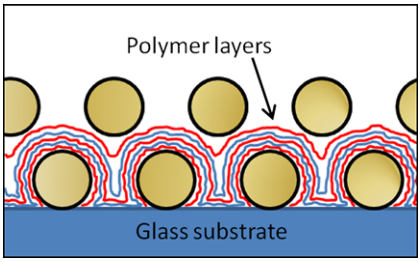

Fig. 1.9 Graphical representation of two gold nanoparticle arrays deposited on a glass substrate and separated by a well-defined number of polyelectrolytes. Adapted with permission from [36]. Copyright (2011) American Chemical Society

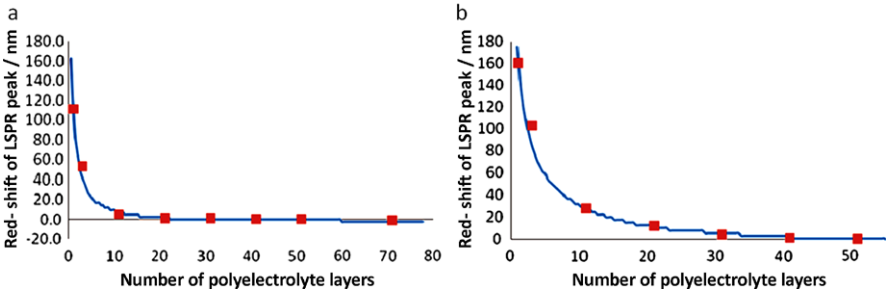

Fig. 1.10 Red-shift upon addition of a second layer of GNPs as a function of layer separation. Both experimental (*squares*) and simulated (*blue solid line*) data are shown for particles of (**a**) 10 nm radius and (**b**) 20 nm radius. Adapted with permission from [36]. Copyright (2011) American Chemical Society

rather than individual nanoparticles, are considered and offers a means of tuning the optical properties of such systems. Further advantages offered by this method include that unlike the Langmuir-Blodgett technique [74], for example, the deposition of polyelectrolytes can be applied to surfaces of virtually any topology and that the deposition occurs extremely quickly, over a period of seconds. In addition, similarly to the size of the initial substrate functionalised, only practical limitations exist both in terms of how many gold nanoparticle arrays are deposited and their relative separations. This, along with the flexibility that is offered, whereby a variety of different sample architectures can be conceived, all adds to the versatility of the method.

When two gold nanoparticle arrays are fabricated in such a manner that they are separated by well-defined distances, the magnitude of the dominant resonance is strongly dependent on the extent of that separation. This can be seen in Fig. 1.10a which shows the red-shift of the LSPR that is induced upon the deposition of a second gold nanoparticle array (both comprised of gold nanoparticles of radius 10 nm) as a function of the number of polyelectrolyte layers that separate them [36]. The red-shift is seen to decrease with increasing layer separation until the particles are moved outwith the coupling limit. An excellent agreement is observed between experimental (squares) and simulated (solid line) results.

Figure 1.10b also shows the effect that particle size has on systems such as these with larger particles, of 20 nm radius, being used to fabricate the same structure. It can be seen that the interaction between particles, as would be expected from the-

oretical studies [75], is even stronger and extends further for larger particles. This is a result of coupling limits essentially being a function of particle size. A more pronounced red-shift is observed for comparable separations when larger particles are used. Again, an excellent agreement between experimental (squares) and simulations (solid line) exists. Additionally, it can be seen that in this case, larger separations are required to shift the distinct arrays of particles outwith the coupling limits. This further increase of polyelectrolyte layers results in a reduction of the interaction of the gold nanoparticles and the optical response should again be dominated by that of a single particle with no observable red-shift. In addition to being affected by inter-particle coupling the LSPR that is exhibited by the gold nanoparticle arrays is also influenced by changes in the refractive index of the surrounding medium. An overall increase in dielectric constant results in the peak position shifting to higher wavelengths [76] in an effect that decreases exponentially from the surface of the particles [75]. As such the resonance frequency will shift upon the deposition of the polyelectrolyte layers themselves [36], an effect that should be taken into account when considering the resulting changes in optical properties observed upon the deposition of additional gold nanoparticle arrays.

All of the techniques, outlined in previous sections, that allow a great degree of control over the filling fraction of the particles deposited directly on a substrate, remain equally applicable to subsequent arrays that have been deposited on polyelectrolyte layers. This adds to the flexibility offered by such fabrication techniques, one of the major advantages of bottom-up technologies.

1.2.6 Observation of Plasmon Splitting

As outlined in the Introduction, the coupling of two spheres can be described with the principles of plasmon hybridisation theory, shown schematically in Fig. 1.1. The addition of a second array of gold nanoparticles results in a splitting of the single resonance into two, where the dominant one is strongly red-shifted. As the optical response within a single GNP layer was dominated by the LSPR of a single sphere, this red-shifted resonance is governed by the mutual coupling of spheres from distinct GNP layers.

When GNP array separation is extremely small, for example by depositing only a single polyelectrolyte layer between two arrays, a rather amorphous structure containing a variety of dimer orientations relative to the incident wave vector results. In such a configuration, all of the bonding and antibonding eigenmodes can be excited [77]. Importantly, only the eigenmodes with a resulting dipole moment dominate the extinction spectra. As a consequence, both such modes should be simultaneously excited and the LSPR should split into two individual and resolvable resonances. This has been both observed experimentally and predicted by simulation as can be seen in Fig. 1.11 [36]. The simulated trace is shown (dashed line, right-hand axis) in addition to both the measured optical response from a single array of GNPs (lower solid line, left-hand axis) and the splitting is observed when a second layer of GNPs is deposited with only one polyelectrolyte separating layer between (upper

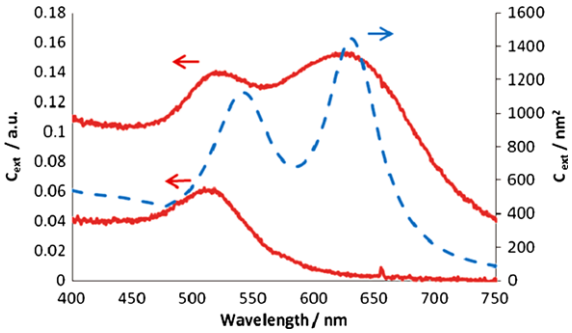

Fig. 1.11 Evolution of longitudinal plasmon peak at shorter GNP (radius 10 nm) layer separations. Shown are the optical responses of a single array of GNPs measured on a glass substrate (*lower solid line, left-hand axis*) and both the experimental (*left-hand axis, upper solid line*) and simulated (*right-hand axis, dashed line*) spectra of a double array of GNPs with one separating polyelectrolyte layer. Adapted with permission from [36]. Copyright (2011) American Chemical Society

solid line, left-hand axis). Both eigenmodes with a resulting dipole moment, π^* and σ (Fig. 1.1), can be observed with the $\pi^*(\sigma)$ coupled plasmon being observed at shorter (longer) wavelengths.

1.2.7 Asymmetric Arrays of Metallic Nanoparticles

One of the more recent applications of plasmonic nanostructures can be found in the field of metamaterials where they are increasingly being used to facilitate the down-scaling of structures that exhibit properties such as a dispersive permeability [78, 79] or permittivity that are exploited for cloaking applications [80] and negative refractive index materials. Such down-scaling is necessary if these properties are going to be routinely observed and utilised at optical frequencies. The dark eigenmodes described in the introduction to this chapter play an important role in this field as the out of phase oscillation of electric dipoles can be related in some cases to a magnetic dipole moment which is the key component in many predicted applications of metamaterials.

One way to excite dark eigenmodes is to use structures that exhibit a considerable amount of asymmetry. The majority of studies of metallic nanoparticles which show asymmetry in either size, shape, or composition has been limited to discussions, both theoretical [81–83] and experimental [84], relating to interactions between low numbers of isolated particles. However in an extension to the work with gold nanoparticles outlined in previous sections [36], it has been shown that it is possible to fabricate large-scale arrays of metallic nanoparticles which display sufficient asymmetry to allow one to excite these dark modes. A net dipole moment is now displayed in each of the four modes shown in Fig. 1.1, meaning that all modes

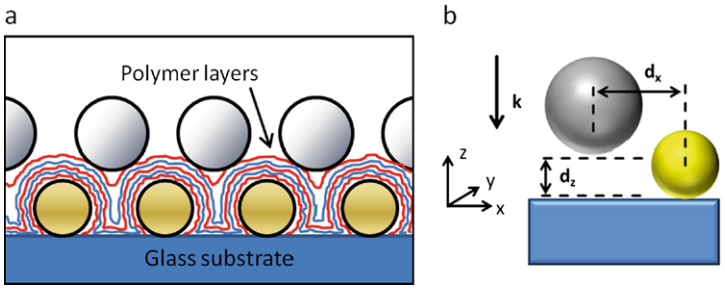

Fig. 1.12 (**a**) Schematic representation of the structure under study showing Au and Ag nanoparticle arrays separated by several polyelectrolyte layers of alternating charge. (**b**) Structure under investigation in the simulations consisting of a heterodimer of one Au and one Ag nanoparticle. The structure is illuminated by a plane wave propagating along the z direction. Geometrical parameters and polarisation of the incident field are described in the text

can be excited at normal incidence, unlike in the system constructed with homoarrays of nanoparticles. Strongly coupled gold and silver nanoparticle arrays induce the required asymmetry due to the shifted LSPR frequencies of the nanoparticles of different composition.

A representation of the principal structure under study in the experimental work is shown in Fig. 1.12a. The two strongly coupled metallic nanoparticle arrays, deposited sequentially on a substrate are separated by an odd integral number of polyelectrolyte layers. Simulations related to this work were performed on an arrangement of two nanoparticles, which could also be considered as a heterodimer, the geometrical configuration of which is shown in Fig. 1.12b.

The silver nanoparticles are prepared in a manner very similar to that of the gold nanoparticles, using a technique known as the Lee-Meisel method [85]. Essentially, a solution of silver salt is reduced by the addition of sodium citrate, which then additionally caps the particles, thus inducing a negative surface charge. Silver nanoparticles produced by the Lee-Meisel method exhibit a wider range of particle sizes and shapes, and do not form as homogeneous an array when deposited on a substrate when compared to the Turkevich method used for gold nanoparticles. This renders the spectral interpretation of the ensembles more challenging. However, the dominating resonances of the system can be fully described by considering a dimer consisting of one gold nanoparticle and one silver nanoparticle from each array, as shown in Fig. 1.12b. Therefore, the identification of peaks that correspond uniquely to the interaction between the distinct arrays of gold and silver nanoparticles and the detection of dark modes is possible for the structure under investigation.

Figure 1.13a depicts the measured extinction spectra for gold and silver nanoparticle arrays separated by a range of different numbers of polyelectrolyte layers. Two resonances with distinct spectral behaviour are observed. The resonance at longer wavelengths is shifted to the red for a decreasing number of separating polyelectrolyte layers. Furthermore, the peak amplitude of this resonance stays nearly constant. Conversely, the resonance at shorter wavelengths offers a nearly constant resonance position whereas the peak amplitude depends on the number of polyelec-

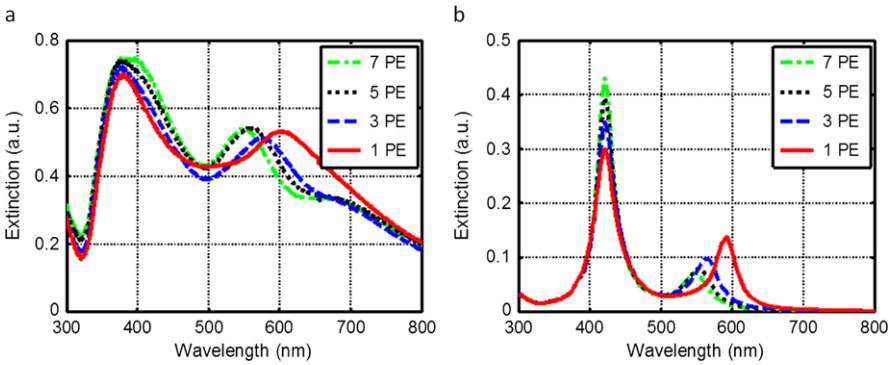

Fig. 1.13 (**a**) Measured and (**b**) simulated extinction spectra for strongly coupled gold–silver nanoparticle layers for different numbers of separating polyelectrolyte layers

trolyte layers. Increasing the number of polyelectrolyte layers, thus decreasing the coupling between particles, results in an enhancement of the peak amplitude. There is an additional resonance, which can be identified just below 700 nm, present in the experimental spectra which results from small aggregates in the silver nanoparticle array. This band, however, does not contribute to one of the four hybridised resonances, shown in Fig. 1.1, that result from the mixing and splitting of modes when two nanoparticle arrays are brought together and can therefore be neglected from subsequent discussions.

The results of the numerical simulations are shown in Fig. 1.13b. The qualitative behaviour of the two resonances as observed in the experiments is entirely reproduced in the simulations. Both simulations and experiments show an increasing peak amplitude for a greater array separation, or in other words, a reduced coupling of the spheres. One explanation of this trend could be the excitation of a dark eigenmode at this wavelength. If the particles are strongly coupled, the eigenmode cannot radiate into the far-field and therefore the amplitude of the extinction is suppressed. If the coupling is reduced the excitation into the far-field is increased and therefore the amplitude of the peak extinction should be enhanced, as is observed in both experiments and simulations.

To facilitate a clear identification of the excited eigenmodes of the structure and to reveal their properties in terms of the hybridisation scheme, shown in Fig. 1.1, the simulated results of the heterodimer can be further interpreted. In Mie theory, one has direct access to all excited multipole moments of every sphere in a system of spheres that is illuminated by an incident field. The reason is that the scattered fields of all spheres involved are decomposed into the eigenfuntions of the Helmholtz equation and this expansion is comparable to a multipole expansion in spherical coordinates. Therefore, the excited electric dipole moments, and their phase relation to each other, of the two spheres of the simulated heterodimer can be revealed directly from Mie theory. A detailed discussion can be found in Refs. [86] and [87]. Sketches of the electric dipoles at the two resonance positions for a single separating polyelectrolyte layer are shown in Fig. 1.14c and Fig. 1.14d.

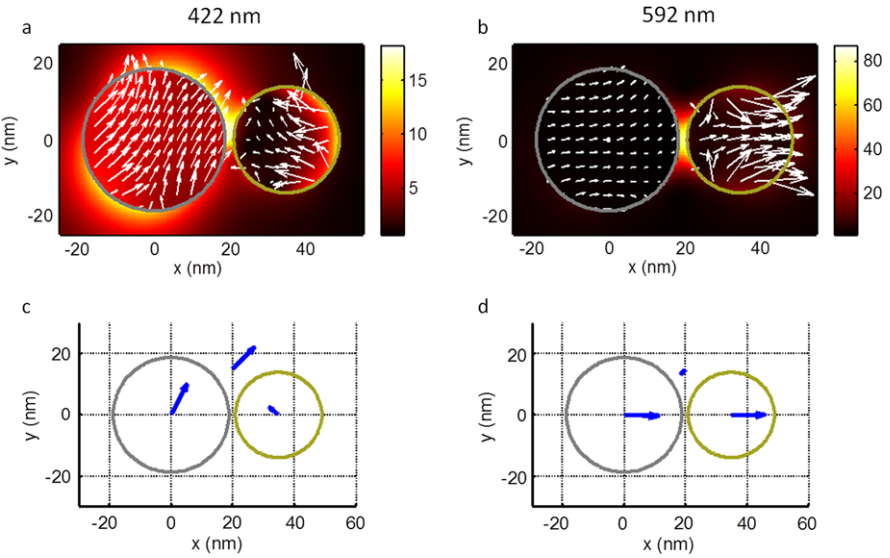

Fig. 1.14 Illustration of the asymmetric (**a**, **c**) and symmetric (**b**, **d**) eigenmodes for the dimer structure separated by one polyelectrolyte layer. (**a**) and (**b**) show the magnitude of the electric field (normalised to the incident field) for both resonances as well as the vectorial character of the internal fields. The lengths of the *white arrows* decode the magnitude of the internal field at this position and the direction shows the contribution of the x- and the y-component of the internal field to its magnitude. (**c**) and (**d**) depict the excited electric dipoles at both resonances of the gold and the silver sphere as they contribute to the scattered field. These dipoles are sketched as *blue arrows* coinciding with the origin of the respective sphere. The *third arrow* (at $x = 20$ nm) shows the polarisation of the incident field at the respective time where the snapshot is taken. All xy-cross sections shown include the centre of the gold sphere. One polyelctrolyte layer, as defined in Fig. 1.12b and in the text, has been chosen to separate the particles. Illumination is in the z-direction, i.e. normal to the plane shown

For the long wavelength resonance, shown in Fig. 1.14d, the in-phase oscillation of the electric dipoles is clearly observed which indicates the excitation of the bright σ eigenmode. However, the excited electric dipoles are not strictly oscillating along the connection line of the spheres, but are also rotating around the origin of the spheres. This is an effect of the polarisation of the incident field which is parallel to a diagonal in the xy-plane. This excited eigenmode is dominated by an in-phase oscillation of both electric dipoles and is therefore a bright mode. In addition, as is well-known for σ eigenmodes of dimers, the electric field is largely enhanced in-between both spheres as can be seen in Fig. 1.14b which shows the magnitude of the electric field and the vectorial character of the internal electric fields of both spheres. The in-phase oscillation of the σ eigenmode can also be observed. The short wavelength resonance, shown in Fig. 1.14c, offers a completely different picture of the excited dipoles in the silver and the gold sphere. Their oscillation can be understood as an interference of the σ^* and π^* eigenmode from Fig. 1.1. Here, the excited dipoles in Fig. 1.14c are oscillating 180° out of phase along the connec-

tion line of the spheres (the x direction) and in-phase parallel to the connection line (the y direction). This interference is again an effect of the chosen polarisation of the incident field which allows both types of eigenmodes to be excited at the same time. As such, in the experiments, where the dimers exhibit an amorphous orientation, both eigenmodes (σ^* and π^*) should interfere for every heterodimer at this wavelength. The overall behaviour of the eigenmode excited at shorter wavelengths offers an out-of phase oscillation of the electric dipoles of the involved spheres, and is therefore identified as a dark eigenmode. Furthermore, the asymmetric character of this eigenmode is clearly seen in Fig. 1.14a, which shows the magnitude of the electric field and the vectorial internal fields. The explanation, given previously, of the increasing peak amplitude in extinction (see Fig. 1.13) for an increasing number of polyelectrolyte layers is in full agreement with these conclusions.

1.2.8 Core–Shell Nanoclusters

It is not only planar organisations of metallic nanoparticles which are of interest to the metamaterials community. Spherical arrangements, otherwise known as core–shell nanoclusters, have also stimulated a great deal of discussion in the literature, both of a theoretical [47, 78, 80] and experimental [88–90] nature. Such materials have garnered intense interest as they have highly tunable optical properties and it has been proposed that they allow advancements towards materials with double negative properties [78].

The usefulness of such structures to the metamaterials community is largely due to the electromagnetic properties that they possess. As has been already outlined, when two coupled plasmonic nanospheres are considered using the hybridisation model described in Fig. 1.1 both symmetric and antisymmetric hybridised modes result. The antisymmetric resonances are strongly sub-radiant and will be perceived as magnetic dipoles in the far-field. This magnetic response is an important element where many further applications are concerned [91, 92]. While structures with strong magnetic dipolar responses can be fabricated by top-down techniques [93, 94], the disadvantages which this entails, not least of which are the difficulties involved in creating bulk materials and assigning effective material parameters, indicate that bottom-up techniques should, at least, be considered as a means of making advancements in the field.

While several bottom-up preparative routes resulting in such structures exist [88–90], given all of the advantages related to electrostatic self-assembly outlined in previous sections, perhaps the most facile and flexible method is an extension of that used to construct planar arrays of gold nanoparticles. In a development to techniques that have already been outlined, by replacing the large-scale planar substrates with smaller scale spherical ones it is possible to create solutions of such core–shell nanoclusters. It is also possible to apply the principles described in these syntheses to other systems, for example those including semiconductor and magnetic nanoparticles.

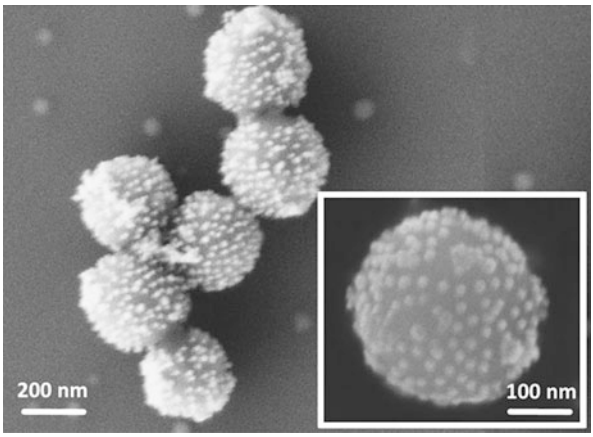

Fig. 1.15 Scanning electron micrographs of fabricated core–shell clusters. An amorphous arrangement of core–shell clusters is shown with the *inset* depicting a zoomed in view showing a single core–shell cluster. Adapted with permission from [79]. Copyright (2011) American Chemical Society

In order to induce the electrostatic attraction between substrate and particle it is first necessary, as before, to functionalise the surface of the substrate. This is regardless of the size or form of the substrate. Fortunately, it is possible to functionalise microspheres of silica using the same reaction as was described in previous sections for planar glass or silicon substrates, albeit under slightly different conditions [79]. This colloidal nanochemistry approach requires additional purification steps, such as centrifugation, however large parallels remain between the two methods. Figure 1.15 shows SEM images of core–shell nanoclusters that have been fabricated by such a method [79].

It can be seen that the dielectric spheres are coated with a large number of isolated, non-touching gold nanoparticles. The organisation of the gold nanoparticles results in large changes in the optical properties when compared to isolated units which are uncoupled to others. This is shown in Fig. 1.16 which highlights both experimental (a) and simulated (b) results [79]. All traces in Fig. 1.16 are normalised to their respective maxima in the region under study.

Immediately apparent in the experimental spectra shown in Fig. 1.16a is the large red-shift, from around 520 nm to around 670 nm, of the LSPR that is induced upon the organisation of the gold nanoparticles, shown as solid red traces, into a spherical geometry, depicted in the extinction spectra as dashed blue traces. This is in excellent agreement with the simulated spectra shown in Fig. 1.16b where the extent of the red-shift is reproduced almost exactly. Any slight deviations could be explained by the fact that in the simulations only a single core–shell nanocluster is considered, compared to the situation in the case of the experimental work where a large ensemble in solution are measured spectroscopically. Here, there will be a certain degree of polydispersity in relation to both the dielectric core and metallic shell spheres. Additionally the organisation of the metallic nanoparticles, while to a large extent comparable, is not identical on each of the individual structures. These slight differences in geometrical parameters can clearly not be taken into account in a simulation of a solitary core–shell nanocluster. Despite any discrepancy between the experimental and simulated spectra, with respect to the strongly red-shifted res-

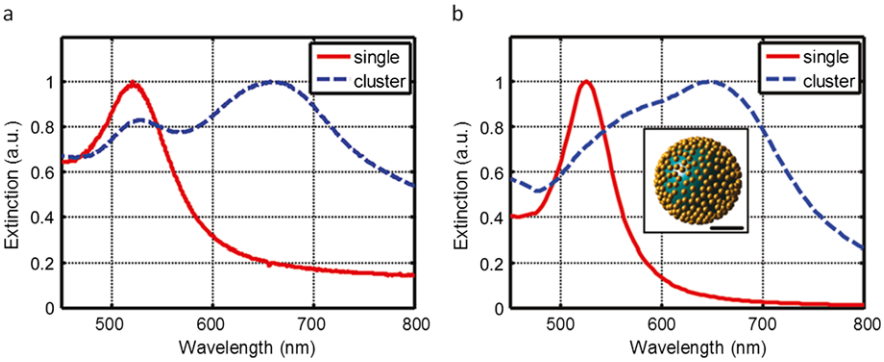

Fig. 1.16 (**a**) Measured extinction spectrum of fabricated core–shell clusters in solution (*blue dashed trace*). For comparison, the extinction spectrum of a solution of gold nanospheres is shown (*red solid trace*). (**b**) Simulated extinction spectra of core–shell clusters in solution (*blue dashed trace*) and a single gold nanosphere (*red solid trace*). The *inset* shows a sketch of the structure under investigation (*scale bar* = 100 nm). Adapted with permission from [79]. Copyright (2011) American Chemical Society

onance, the agreement is convincing. However, one major difference between the two traces can be discerned. A peak in the experimental spectra at the same wavelength as the LSPR of an isolated particle is not reproduced in the simulations. This is caused by excess gold nanoparticles in solution which result from the fabrication process. It is thought that to ensure the cores remain covered an excess of 'free' gold nanoparticles must be present. This could be as a result of an equilibrium existing between the gold nanoparticles at the surface of the dielectric cores and those in solution. These particles are not considered in the simulations and account for this difference between the experimental and simulated data.

It has been proposed that such structures exhibit a strong isotropic magnetic response [78]. This magnetism can be explained by assuming that the shell of metallic nanospheres acts, in effect, as a medium with an extremely high permittivity at wavelengths slightly above the collective plasmonic resonance. The large permittivity in turn evokes Mie resonances. For the lowest order one, the electric displacement field rotates in a plane perpendicular to the polarisation of the incident magnetic field, meaning that this mode can be associated with a magnetic dipole contribution. That the core–shell nanoclusters exhibit artificial isotropic magnetism can be confirmed through simulations, which have proven to be in excellent agreement with experimental results, by deconstructing the extinction spectra and examining the contribution of the respective multipole moments to the scattered field of the structures. Further details of this process, which is outwith the scope of this chapter, can be found in Ref. [78].

The fabrication of these structures is extremely flexible and a number of possibilities to fine tune the architecture, and therefore the optical properties, are available. For instance, a wide range of sizes of both the dielectric core and the surrounding gold nanoparticles can be accessed. Additionally, while the fabrication above relates to a coating of gold nanoparticles on a SiO_2 core sphere different elements

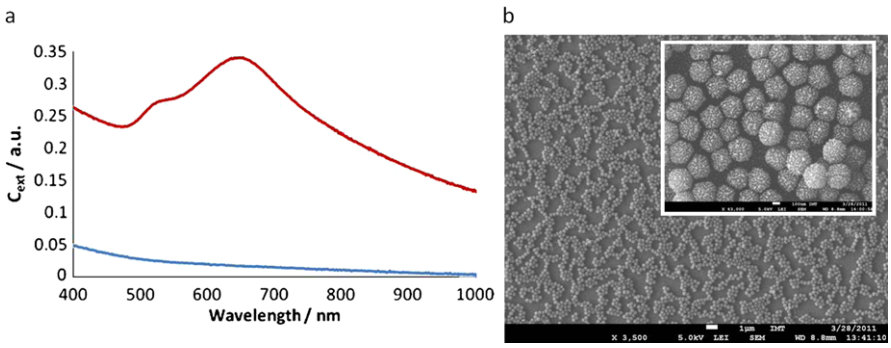

Fig. 1.17 (**a**) Extinction spectra showing an array of SiO_2 microshperes deposited on a charged glass substrate both pre- (*blue trace*) and post- (*red trace*) functionalisation with gold nanoparticles. (**b**) SEM micrographs of an array of core–shell nanoclusters deposited on a charged silicon substrate

can be brought together in a similar manner. Structures using polymer, or metallic, core spheres coated with nanoparticles of a variety of different materials and functionalities can be envisaged. The only prerequisite for their fabrication is that an attraction, of either a physical or chemical nature, exists between the two. In this work the widespread applicability of electrostatic interactions has been highlighted.

This electrostatic approach can also be used to produce large-scale arrays of core–shell nanoclusters deposited on planar substrates. Such a step is required if systems like this are to be incorporated into functional optical devices. In addition, pre-depositing functionalised SiO_2 cores on a planar substrate prior to their coating with metallic nanoparticles could prove to be a promising route to reducing or eliminating the excess particles in solution which existed in the previous fabrication approach. Shown in Fig. 1.17a are extinction spectra which again highlight the possibilities of creating systems with tunable optical properties simply through the organisation and ordering of metallic nanoparticles. The lower, blue, trace corresponds to a single layer of silica microspheres which have been adsorbed on a substrate. The deposition of the spheres, which are charged positively after a functionalisation step, self-assemble at the glass substrate surface which has itself been coated in a negatively charged polymer. The upper, red, trace corresponds to the same array of microspheres after gold nanoparticles have been deposited at the surface. The arguments, given previously, for the exhibition of a strong isotropic magnetic response and for the large red-shift of the LSPR, when compared to that of an isolated particle, remain unchanged. However, the large step that has been taken, from structures that exist purely in colloidal form to the formation of large scale single layers show the versatility and applicability of the bottom-up techniques used. The two SEM images shown in Fig. 1.17b give an idea of what is achievable. The larger image shows that arrays can be created on a suitably large scale while the image in the inset shows that, at least in small domains, a degree of order can be achieved. Additionally, it should also be possible to combine such methods with the layer by layer assembly outlined previously, allowing the construction of truly bulk optical materials.

1.3 Conclusions

The examples of bottom-up techniques used to organise metallic nanoparticles into structures with tailored optical properties described in detail in the previous section highlight the process of taking a design and discovering ways to realise it. Additionally, the large extent to which simulations can now be relied upon to give an accurate reflection of the true experimental situation means that these simulations can now be used as an effective design tool, allowing theoreticians to propose structures with desirable properties that can then be realised through chemical methods. In most cases there will exist several fabrication routes, exploiting different interactions of a chemical and physical nature, which will result in the same structure. This fabrication process, where the myriad of combinations that exist mean that, within certain practical limits, possible structures are only really restricted by the imagination. After different fabrication routes have been identified the onus is then placed on the materials scientist to determine which course provides the best scientific results while also taking into consideration other factors such as cost effectiveness and time efficiency.

An attempt has been made to give an introduction to the wide variety of bottom-up fabrication techniques that can be used to organise metallic nanoparticles into structures that could be put to practical use in functional devices or applications. Additionally, an overview of the areas to which nanoparticles such as these can be applied has also been given. The wide range of these applications, from purely decorational through to biomedical and metamaterials, shows the versatility and flexibility of such systems and that they can be put to practical use in a broad array of areas, the full scope of which is yet to be fully realised.

In particular, a wide range of applications could be envisaged for the two systems discussed in more detail in the last section, more specifically in the fields of metamaterials and plasmonics. The extent to which the optical properties of such systems can be tailored to meet particular requirements, as well as the means used to modify them has been described in detail. The flexibility of several material parameters of the structure, whereby metallic nanoparticles of different size, composition and shape can be deposited on functionalised substrates of varying form and the ability to control the distance between them to within almost nanometre precision means that such systems could have roles to play in a variety of different applications. For example, the suitability of the planar arrays of metallic nanoparticles for applications in SERS has been investigated and it has been shown that the distance between the two arrays of particles, which can be controlled by changing the number of polyelectrolyte layers deposited between them, has a large effect on the enhanced Raman signal. As the distance between the two arrays is increased the electromagnetic field focused in the nanogap, which is the principal cause of enhancements observed, decreases and the Raman signal is seen to decrease accordingly.

Alternatively, taking the structure of radio frequency Yagi-Uda antennas as inspiration it has been proposed that the close correspondence between this and the stratified arrays of metallic nanoparticles could give rise to waveguides for single photon and single plasmon sources [95]. Similar comparisons have been drawn in

other publications [96, 97], taking well-developed technology and down-scaling it to achieve nano-scale equivalents with plasmonic inclusions that result in structures that could be included in nanophotonic and nanoelectronic devices. The ability to prepare many layers of metallic nanoparticles with controllable distances between them makes these applications a very real possibility. Taking motivation from other related theoretical studies, nanolenses constructed of chains of nanoparticles progressively diminishing in size and separation could also be made a reality. The focus of this nanolens or 'hottest spot' would exist in the gap separating the two smallest nanoparticles where the electromagnetic fields are further enhanced compared to what is normally seen in a simple dimer due to the multiplicative, cascade effect of its geometry [98]. Other possible applications of the layered arrays of nanoparticles include superlensing, one of the holy grails of metamaterials research, whereby the diffraction limit, which is an inherent limit present in all conventional optical devices, is broken. One of the first experimental observations of superlensing came in 2004 whereby images significantly narrower that those predicted by the diffraction limit were formed [34]. However this work was conducted in the microwave region of the electromagnetic spectrum and as has been outlined throughout this text, the control offered by novel bottom-up techniques permits these structures to be down-scaled and similar properties to be observed in the visible regime.

A massive range of potential sensing applications for such systems also exists. The sensitivity of the LSPR to localised changes in refractive index means that a huge variety of analytes can be accurately and precisely measured. When combined with the almost limitless catalogue of surface chemistry modifications that are accessible which introduces the additional dimension of selectivity. Other cutting edge sensing applications using structures such as the one under discussion could include the incorporation of, for example, thermally responsive polymers, which would result in a plasmonic system with temperature dependent optical properties [99]. Alternatively, by preparing the layered arrays of gold nanoparticles on softer substrates such as PDMS rather than glass or silicon pressure sensors, where the optical response varies with stretching or compression, resulting in a deformation of the nanoparticle organisation and shifts in the optical properties, could be envisaged.

These practical applications are in addition to the pure scientific insight that can be achieved from studying different architectures of gold nanoparticles. As was shown in the detailed study of core–shell nanoclusters [79] they exhibit artificial isotropic magnetism in the visible spectral domain—a key element of many metamaterials applications. One such application is the construction of cloaking devices [80]. It has been shown theoretically that very similar structures to the core–shell nanoclusters shown in the main body of this chapter should, to a certain extent, attenuate the scattering response of the internal dielectric core sphere. For this to be achieved it is necessary for the system to be constructed using relatively small core spheres decorated with silver nanoparticles, whose optical properties are significantly different from their gold counterparts.

This chapter has given a glimpse of what is currently achievable in the field of bottom-up self-assembly of metallic nanoparticle structures with a degree of focus

given to their applicability in the preparation of metamaterials at optical frequencies. Specific methods of creating a wide variety of metallic nanoparticles with a wide range of optical properties have been introduced along with the means to organise them and control their optical properties. These means can be built upon, improved and combined with others to make other structures with exciting possibilities equally achievable. This flexibility, allowing for the inclusion of almost any charged species in the layered arrays of metallic nanoparticles for example, is a signature element of the bottom-up approach and, along with the high degree of control achievable, is one of the major advantages of this approach. Using self-assembly at all levels, from the nanoscale to the macroscale, several material parameters, such as particle composition, size and separation, can be manipulated with impressive precision. In addition, the simplicity and robustness of the approach, coupled with the large-scale of the substrates that can be produced, opens up the possibility of integrating such structures into functional devices and components, which should be the goal if the fruits of such research is to continue having a positive impact on our lives.

Acknowledgement Financial support from the University of Geneva and the European Union FP7 (project NANOGOLD) is kindly acknowledged.

References

1. C. Lok, Nanotechnology: small wonders. Nature **467**(7311), 18–21 (2010)
2. R.P. Feynman, There's plenty of room at the bottom. CALTECH Eng. Sci. **23**(5), 22–36 (1960)
3. S.E. Thompson, S. Parthasarathy, Moore's law: the future of Si microelectronics. Mater. Today **9**(6), 20–25 (2006)
4. X. Li et al., Solar cells and light sensors based on nanoparticle-grafted carbon nanotube films. ACS Nano **4**(4), 2142–2148 (2010)
5. E. Boisselier et al., How to very efficiently functionalize gold nanoparticles by "click" chemistry. Chem. Commun. **2008**(44), 5788–5790 (2008)
6. M. Shimomura, T. Sawadaishi, Bottom-up strategy of materials fabrication: a new trend in nanotechnology of soft materials. Curr. Opin. Colloid Interface Sci. **6**(1), 11–16 (2001)
7. C. Acikgoz et al., Polymers in conventional and alternative lithography for the fabrication of nanostructures. Eur. Polym. J. **47**(11), 2033–2052 (2011)
8. M. Zhu et al., Structural and optical characteristics of silicon nanowires fabricated by wet chemical etching. Chem. Phys. Lett. **511**(1–3), 106–109 (2011)
9. S. Reyntjens, R. Puers, A review of focused ion beam applications in microsystem technology. J. Micromech. Microeng. **11**(4), 287 (2001)
10. H. Zeng et al., Nanomaterials via laser Ablation/Irradiation in liquid: a review. Adv. Funct. Mater. **22**(7), 1333–1353 (2012)
11. N.J. Halas, Plasmonics: an emerging field fostered by nano letters. Nano Lett. **10**(10), 3816–3822 (2010)
12. R. Gans, Form of ultramicroscopic particles of silver. Ann. Phys. **47**, 270 (1915)
13. R. Wilson, The use of gold nanoparticles in diagnostics and detection. Chem. Soc. Rev. **37**(9), 2028–2045 (2008)
14. M.E. Stewart et al., Nanostructured plasmonic sensors. Chem. Rev. **108**(2), 494–521 (2008)
15. M. Fleischmann, P.J. Hendra, A.J. McQuillan, Raman spectra of pyridine adsorbed at a silver electrode. Chem. Phys. Lett. **26**(2), 163–166 (1974)

16. N.J. Halas et al., Plasmons in strongly coupled metallic nanostructures. Chem. Rev. **111**(6), 3913–3961 (2011)
17. G.R. Souza et al., *In vivo* detection of gold-imidazole self-assembly complexes: NIR-SERS signal reporters. Anal. Chem. **78**(17), 6232–6237 (2006)
18. J.M. Romo-Herrera, R.A. Alvarez-Puebla, L.M. Liz-Marzan, Controlled assembly of plasmonic colloidal nanoparticle clusters. Nanoscale **3**, 1304–1315 (2011)
19. R. Jin, Nanoparticle Clusters Light Up in SERS. Angewandte Chemie International Edition **49**(16), 2826–2829 (2010)
20. W. Page Faulk, G. Malcolm Taylor, Communication to the editors: an immunocolloid method for the electron microscope. Immunochemistry **8**(11), 1081–1083 (1971)
21. R.A. Sperling et al., Biological applications of gold nanoparticles. Chem. Soc. Rev. **37**(9), 1896–1908 (2008)
22. Q. Wei, J. Ji, J. Shen, Synthesis of near-infrared responsive gold nanorod/PNIPAAm core/shell nanohybrids via surface initiated ATRP for smart drug delivery. Macromol. Rapid Commun. **29**, 645–650 (2008)
23. D.A. Giljohann et al., Gold nanoparticles for biology and medicine. Angew. Chem., Int. Ed. **49**(19), 3280–3294 (2010)
24. E.C. Dreaden et al., Beating cancer in multiple ways using nanogold. Chem. Soc. Rev. **40**(7), 3391–3404 (2011)
25. C. Sonnichsen et al., A molecular ruler based on plasmon coupling of single gold and silver nanoparticles. Nat. Biotechnol. **23**(6), 741–745 (2005)
26. M. Chen, D.W. Goodman, Catalytically active gold on ordered titania supports. Chem. Soc. Rev. **37**(9), 1860–1870 (2008)
27. J.R. Adleman et al., Heterogenous catalysis mediated by plasmon heating. Nano Lett. **9**(12), 4417–4423 (2009)
28. H. Nabika et al., Toward plasmon-induced photoexcitation of molecules. J. Phys. Chem. Lett. **1**(16), 2470–2487 (2010)
29. C.J. Chen, R.M. Osgood, Direct observation of the local-field-enhanced surface photochemical reactions. Phys. Rev. Lett. **50**(21), 1705–1708 (1983)
30. T. Arakawa et al., Effects of silver nanoparticles on photoelectrochemical responses of organic dyes. J. Phys. Chem. C **113**(27), 11830–11835 (2009)
31. D.R. Smith et al., Composite medium with simultaneously negative permeability and permittivity. Phys. Rev. Lett. **84**(18), 4184–4187 (2000)
32. R.A. Shelby, D.R. Smith, S. Schultz, Experimental verification of a negative index of refraction. Science **292**(5514), 77–79 (2001)
33. D. Rainwater et al., Experimental verification of three-dimensional plasmonic cloaking in free-space. New J. Phys. **14**(1), 013054 (2012)
34. A. Grbic, G.V. Eleftheriades, Overcoming the diffraction limit with a planar left-handed transmission-line lens. Phys. Rev. Lett. **92**(11), 117403 (2004)
35. E. Prodan et al., A hybridization model for the plasmon response of complex nanostructures. Science **302**(5644), 419–422 (2003)
36. A. Cunningham et al., Coupling of plasmon resonances in tunable layered arrays of gold nanoparticles. J. Phys. Chem. C **115**(18), 8955–8960 (2011)
37. X. Zeng, 3D ordered gold strings by coating nanoparticles with mesogens. Adv. Mater. **21**, 1746 (2009)
38. H. Qi et al., Effects of hydrophilic and hydrophobic gold nanoclusters on the stability and ordering of bolaamphiphilic liquid crystals. J. Mater. Chem. **17**(20), 2139–2144 (2007)
39. R. Pratibha, W. Park, I.I. Smalyukh, Colloidal gold nanosphere dispersions in smectic liquid crystals and thin nanoparticle-decorated smectic films. J. Appl. Phys. **107**(6), 063511 (2010)
40. A.P. Alivisatos et al., Organization of 'nanocrystal molecules' using DNA. Nature **382**(6592), 609–611 (1996)
41. D.D.-K. Lim, Nanogap-engineerable Raman-active nanodumbbells for single-molecule detection. Nat. Mater. **9**(1), 60 (2010)

42. C.-L. Chen, P. Zhang, N.L. Rosi, A new peptide-based method for the design and synthesis of nanoparticle superstructures: construction of highly ordered gold nanoparticle double helices. J. Am. Chem. Soc. **130**(41), 13555–13557 (2008)
43. Nie et al., "Supramolecular" assembly of gold nanorods end-terminated with polymer "pom-poms": effect of pom-pom structure on the association modes. J. Am. Chem. Soc. **130**(11), 3683–3689 (2008)
44. P.K. Jain, S. Eustis, M.A. El-Sayed, Plasmon coupling in nanorod assemblies: optical absorption, discrete dipole approximation simulation, and exciton-coupling model. J. Phys. Chem. B **110**(37), 18243–18253 (2006)
45. E.V. Shevchenko et al., *Structural Diversity in Binary Nanoparticle Superlattices* (Nature Publishing Group, London, 2006), pp. 55–59
46. X. Wang et al., Polymer-encapsulated gold-nanoparticle dimers: facile preparation and catalytical application in guided growth of dimeric ZnO-nanowires. Nano Lett. **8**(9), 2643–2647 (2008)
47. C. Rockstuhl et al., Design of an artificial three-dimensional composite metamaterial with magnetic resonances in the visible range of the electromagnetic spectrum. Phys. Rev. Lett. **99**(1), 017401 (2007)
48. N. Shalkevich et al., Reversible formation of gold nanoparticle-surfactant composite assemblies for the preparation of concentrated colloidal solutions. Phys. Chem. Chem. Phys. **11**(43), 10175–10179 (2009)
49. S. Mühlig et al., Optical properties of a fabricated self-assembled bottom-up bulk metamaterial. Opt. Express **19**(10), 9607–9616 (2011)
50. J.H. Lee, Q. Wu, W. Park, Metal nanocluster metamaterial fabricated by the colloidal self-assembly. Opt. Lett. **34**(4), 443–445 (2009)
51. V. Myroshnychenko et al., Modelling the optical response of gold nanoparticles. Chem. Soc. Rev. **37**(9), 1792–1805 (2008)
52. I. Freestone, The lycurgus cup—a Roman nanotechnology. Gold Bull. **40**(4), 270–277 (2007)
53. M. Faraday, The bakerian lecture: experimental relations of gold (and other metals) to light. Philos. Trans. R. Soc. Lond. **147**, 145–181 (1857)
54. M. Brust et al., Synthesis of thiol-derivatised gold nanoparticles in a two-phase liquid-liquid system. J. Chem. Soc., Chem. Commun. **7**, 801–802 (1994)
55. S.J. Tan et al., Building plasmonic nanostructures with DNA. Nat. Nanotechnol. **6**(5), 268–276 (2011)
56. M. Rycenga et al., Controlling the synthesis and assembly of silver nanostructures for plasmonic applications. Chem. Rev. **111**(6), 3669–3712 (2011)
57. L. Jiang et al., Patterning of plasmonic nanoparticles into multiplexed one-dimensional arrays based on spatially modulated electrostatic potential. ACS Nano **5**(10), 8288–8294 (2011)
58. J.K. Gansel et al., Gold helix photonic metamaterial as broadband circular polarizer. Science **325**(5947), 1513–1515 (2009)
59. C.M. Soukoulis, M. Wegener, Optical metamaterials—more bulky and less lossy. Science **330**(6011), 1633–1634 (2010)
60. K.L. Kelly et al., The optical properties of metal nanoparticles: the influence of size, shape, and dielectric environment. J. Phys. Chem. B **107**(3), 668–677 (2002)
61. J. Schmitt et al., Metal nanoparticle/polymer superlattice films: fabrication and control of layer structure. Adv. Mater. **9**(1), 61–65 (1997)
62. Z. Feng, F. Yan, Preparation and tribological studies of nanocomposite films fabricated using spin-assisted layer-by-layer assembly. Surf. Coat. Technol. **202**(14), 3290–3297 (2008)
63. B.V. Enustun, J. Turkevich, Coagulation of colloidal gold. J. Am. Chem. Soc. **85**(21), 3317–3328 (1963)
64. J. Kimling et al., Turkevich method for gold nanoparticle synthesis revisited. J. Phys. Chem. B **110**(32), 15700–15707 (2006)
65. R.K. Iler, *The Chemistry of Silica: Solubility, Polymerization, Colloid and Surface Properties and the Biochemistry* (Wiley, New York, 1979)

66. M.D. Abràmoff, P.J. Magalhães, S.J. Ram, Image processing with image. J. Biophotonics Int. **7**, 7 (2004)
67. J. Dintinger et al., A bottom-up approach to fabricate optical metamaterials by self-assembled metallic nanoparticles. Opt. Mater. Express **2**(3), 269–278 (2012)
68. D.J. Shaw, *Introduction to Colloid and Surface Chemistry* (Elsevier, Amsterdam, 1989)
69. J.C. Love et al., Self-assembled monolayers of thiolates on metals as a form of nanotechnology. Chem. Rev. **105**(4), 1103–1170 (2005)
70. S.D.T. Brown, B.F.G. Johnson, Nucleation and growth of nano-gold colloidal lattices. Chem. Commun. **11**, 1007–1008 (1997)
71. G. Decher, Fuzzy nanoassemblies: toward layered polymeric multicomposites. Science **277**(5330), 1232–1237 (1997)
72. P. Lavalle et al., Dynamic aspects of films prepared by a sequential deposition of species: perspectives for smart and responsive materials. Adv. Mater. **23**(10), 1191–1221 (2011)
73. A. Tronin, Ellipsometry and x-ray reflectometry characterization of self-assembly process of polystyrensulfonate and polyallylamine. Colloid Polym. Sci. **272**, 1317–1321 (1994)
74. X. Chen et al., Langmuir–Blodgett patterning: a bottom–up way to build mesostructures over large areas. Acc. Chem. Res. **40**(6), 393–401 (2007)
75. A.M. Funston et al., Plasmon coupling of gold nanorods at short distances and in different geometries. Nano Lett. **9**(4), 1651–1658 (2009)
76. G.A. Ozin, A.C. Arsenault, *Nanochemistry—A Chemical Approach to Nanomaterials* (RSC Publishing, Cambridge, 2005)
77. A. Christ et al., Symmetry breaking in a plasmonic metamaterial at optical wavelength. Nano Lett. **8**(8), 2171–2175 (2008)
78. C.R. Simovski, S.A. Tretyakov, Model of isotropic resonant magnetism in the visible range based on core–shell clusters. Phys. Rev. B **79**(4), 045111 (2009)
79. S. Mühlig et al., Self-assembled plasmonic core–shell clusters with an isotropic magnetic dipole response in the visible range. ACS Nano **5**(8), 6586–6592 (2011)
80. S. Mühlig et al., Cloaking dielectric spherical objects by a shell of metallic nanoparticles. Phys. Rev. B **83**(19), 195116 (2011)
81. O. Peña-Rodríguez et al., Enhanced Fano resonance in asymmetrical Au: Ag heterodimers. J. Phys. Chem. C (2011)
82. G. Bachelier et al., Fano profiles induced by near-field coupling in heterogeneous dimers of gold and silver nanoparticles. Phys. Rev. Lett. **101**(19), 197401 (2008)
83. E.R. Encina, E.A. Coronado, On the far field optical properties of Ag-Au nanosphere pairs. J. Phys. Chem. C **114**(39), 16278–16284 (2010)
84. L.V. Brown et al., Heterodimers: plasmonic properties of mismatched nanoparticle pairs. ACS Nano **4**(2), 819–832 (2010)
85. P.C. Lee, D. Meisel, Adsorption and surface-enhanced Raman of dyes on silver and gold sols. J. Phys. Chem. **86**(17), 3391–3395 (1982)
86. C. Rockstuhl et al., Scattering properties of meta-atoms. Phys. Rev. B **83**(24), 245119 (2011)
87. S. Mühlig et al., Multipole analysis of meta-atoms. Metamaterials **5**(2–3), 64–73 (2011)
88. F. Caruso et al., Multilayer assemblies of silica-encapsulated gold nanoparticles on decomposable colloid templates. Adv. Mater. **13**(14), 1090–1094 (2001)
89. B. Sadtler, A. Wei, Spherical ensembles of gold nanoparticles on silica: electrostatic and size effects. Chem. Commun. **15**, 1604–1605 (2002)
90. I. Pastoriza-Santos et al., Optical properties of metal nanoparticle coated silica spheres: a simple effective medium approach. Phys. Chem. Chem. Phys. **6**(21), 5056–5060 (2004)
91. J.B. Pendry, Negative refraction makes a perfect lens. Phys. Rev. Lett. **85**(18), 3966–3969 (2000)
92. U. Leonhardt, T.G. Philbin, Transformation optics and the geometry of light, in *Progress in Optics*, ed. by E. Wolf, 1st edn. (Elsevier, Amsterdam, 2009)
93. C. Enkrich et al., Magnetic metamaterials at telecommunication and visible frequencies. Phys. Rev. Lett. **95**(20), 203901 (2005)

94. J. Valentine et al., Three-dimensional optical metamaterial with a negative refractive index. Nature **455**(7211), 376–379 (2008)
95. A.F. Koenderink, Plasmon nanoparticle array waveguides for single photon and single plasmon sources. Nano Lett. **9**(12), 4228–4233 (2009)
96. A. Manjavacas, F.J. Garcí a de Abajo, Robust plasmon waveguides in strongly interacting nanowire arrays. Nano Lett. **9**(4), 1285–1289 (2008)
97. N. Engheta, Circuits with light at nanoscales: optical nanocircuits inspired by metamaterials. Science **317**(5845), 1698–1702 (2007)
98. K. Li, M.I. Stockman, D.J. Bergman, Self-similar chain of metal nanospheres as an efficient nanolens. Phys. Rev. Lett. **91**(22), 227402 (2003)
99. M. Karg et al., Nanorod-coated PNIPAM microgels: thermoresponsive optical properties. Small **3**(7), 1222–1229 (2007)

http://www.springer.com/978-3-642-32474-1

Amorphous Nanophotonics
Rockstuhl, C.; Scharf, T. (Eds.)
2013, XVIII, 372 p. 264 illus., 98 illus. in color.,
Hardcover
ISBN: 978-3-642-32474-1